

WC-5Co CEMENTED CARBIDES FABRICATED BY SPS

New graphite tools were designed and produced to fabricate a semi-finished product from which nine cutting inserts were obtained in one spark plasma sintering process. As a result, WC-5Co cemented carbides were spark plasma sintered and the effect of various sintering parameters such as compacting pressure, heating rate and holding time on the main mechanical properties were investigated. It was shown that WC-5Co cemented carbides spark plasma sintered at 1200°C, 80 MPa, 400°C/min, for 5 min are characterized by the best relation of hardness ($1861 \pm 10 \text{ HV}_{30}$) and fracture toughness ($9.30 \text{ MPa}\cdot\text{m}^{1/2}$). The microstructure of these materials besides the WC ceramic phase and Co binder phase consists of a synthesized $\text{Co}_3\text{W}_3\text{C}$ complex phase. Comparison with a commercial WC-6Co cutting insert fabricated by conventional powder metallurgy techniques shows that spark plasma sintering is a very effective technique to produce materials characterized by improved mechanical properties.

Keywords: spark plasma sintering, cemented carbides, WC-5Co, hardness, fracture toughness

1. Introduction

Tungsten carbide-cobalt (WC-Co) cemented carbides, in view of some of their excellent properties such as a high hardness, toughness and wear-resistance, are still the most frequently used materials in mechanical engineering mainly as cutting, machining and drilling tools [1-3]. The impact and wear resistance of these tools depend directly on the hardness and fracture toughness of WC-Co cemented carbides. These fundamental properties in turn depend on the microstructure. What is important, according to the Hall-Petch relation [4,5], the hardness of WC-Co cemented carbides increases with a decreasing grain size. Hence, ultrafine and nanocrystalline microstructures are the most appropriate [6]. Unfortunately, the fracture toughness is inversely proportional to the grain size, that is why a finer microstructure usually results in a lower fracture toughness [7,8]. Therefore, the key issue is to find an appropriate balance between the hardness and fracture toughness of WC-Co cemented carbides. Currently, most efforts are focused on sintering WC-Co cemented carbides with simultaneously high hardness and high fracture toughness. One of the possibilities is to use non-conventional sintering techniques, e.g. spark plasma sintering (SPS). Many comparative studies have proved the superiority of this technique over conventional sintering to produce WC-Co cemented carbides [9-11]. Owing to the possibility of using a wide range of process parameters, the SPS technique allows one to develop the microstructure and properties of WC-Co cemented carbides. By analyzing the parameters of the SPS process used by many

authors [6,11-44] to fabricate WC-Co cemented carbides, it was found that the sintering temperature ranged between 600 and 1600°C, heating rate between 100 and 600°C/min, compacting pressure between 25 and 100 MPa and the holding time ranged between 0 and 10 min. A few authors [19,26,33,40] also reported the time of pulse on (from 10 to 12 ms) and pulse off (from 2 to 5 ms). Summarizing, a sintering temperature below 1100°C is suitable only for SPS nanometric WC-Co powders [34]. Ultrafine and coarse WC-Co powders should be SPSed at higher temperature. Of course if the sintering temperature is lower, the compacting pressure should be higher, e.g. 1000°C, 100 MPa [16,41] and 1300°C, 75 MPa [31,37].

In this paper, the effect of various parameters of SPS process such as compacting pressure, heating rate and holding time on the main mechanical properties was investigated and the goal of this research work was to produce WC-5Co cemented carbides with high hardness and fracture toughness, which could be a candidate as material for cutting inserts with a long service life.

2. Materials and methods

A WC-5Co (wt%) powder mixture (purity 99.9%) supplied by Metal-Vis was spark plasma sintered using an HP D 25-3 (FCT Systeme) furnace. The sintering temperature of 1200°C was reached at the heating rates (HR) of 200 and 400°C/min and was kept for the holding times (HT) of 5 and 10 min. Compacting pressures (CP) of 50 and 80 MPa were applied throughout the

* USŁUGI SLUSARSKIE, 147A OSTROWSKA STR., 63-405 SIERSZEWICE, POLAND

** METAL FORMING INSTITUTE, 14 JANA PAWŁA II STR., 61-139 POZNAŃ, POLAND

Corresponding author: dariusz.garbiec@inop.poznan.pl

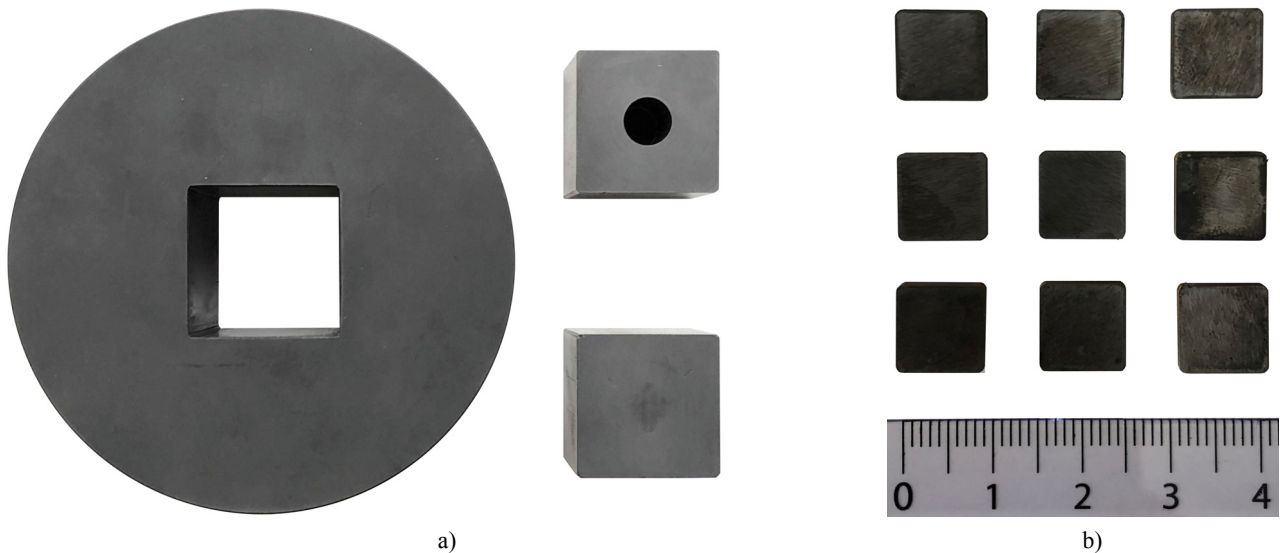


Fig. 1. Photograph of (a) graphite tools and (b) cutting inserts

sintering process. The ratio of pulse on:off time was 12:3, in ms. The pressure level in the sintering chamber was set at 0.05 mbar. The new graphite tools with a hole of a width and depth of 29.8 mm (Fig. 1a) were used to fabricate WC-5Co cemented carbides and then nine square shaped samples with the length and width of 9.7 mm and thickness of ~3.2 mm (Fig. 1b) were cut from the obtained semi-finished products by wire electrical discharge machining (WEDM) for property measurements and microscopic observations. The reference material was an H10 (Sandvik) cutting insert from the ISO K10 group having a similar composition (WC-6Co) fabricated by conventional powder metallurgy techniques.

The particle size distribution of the powder mixture was measured by the laser diffraction method using a Mastersizer 3000 (Malvern) analyzer. The density was measured by the Archimedes method in accordance with the PN-EN ISO 3369:2010 standard using an EX225DM (Ohaus) scale. The hardness was measured by the Vickers method in accordance with the PN-EN 23878:1996 standard using an FV-700 (Future-Tech) hardness tester by applying a load of 294.2 N for 7 s. The Vickers indentation fracture toughness test was used to estimate the K_{Ic} using formula (1) [45], where K_{Ic} is the fracture toughness in $\text{MPa}\cdot\text{m}^{1/2}$, HV_{30} is the Vickers hardness measured under the load of 294.2 N, l is length of the crack from the corner of the indenter in μm .

$$K_{Ic} = \sqrt{\frac{HV_{30}}{\sum_{i=1}^4 l_i}} \quad (1)$$

X-ray structural studies were performed using an Empyrean (PANalytical) diffractometer using $\text{CuK}\alpha$ radiation, Ni filter and the step scan mode. The crystallite size was estimated by the Sherrer method using Highscore (PANalytical) software. Microstructure observations were performed by scanning electron microscopy (SEM) using a Quanta 250 FEG (FEI) microscope equipped with EDS analyser for material composition determination.

3. Results and discussion

Fig. 2 shows the morphology and particle size distribution of the WC-5Co powder mixture. The particles of this powder mixture are generally rounded in shape and occur in the form of agglomerates. The EDS spectra showed that the WC particles are covered with Co probably due to long mixing/milling time of the initial powders. The median of the diameter (D_{50}) of the powder particles measured using the laser diffraction technique is 8.32 μm . The D_{10} and D_{90} values are 5.49 and 17.17 μm , respectively. Direct comparison of the SEM and laser diffraction results reveal that the obtained values of the D_{10} , D_{50} and D_{90} are slightly overstated. It is probably related to insufficient break-down of the agglomerates by ultrasonics before the measurement. Unfortunately, increasing the time of this stage does not generate significantly improvement. The X-ray diffraction results of the powder mixture show that besides the hexagonal WC ceramic (ICDD 01-073-9874) and cubic Co binder (ICDD 01-077-7455) phase, no secondary phases are present. The WC crystallite size of the powder mixture estimated by the Sherrer method is 22 nm.

The results of the density measurements of SPSed WC-5Co cemented carbides are listed in Table 1. All the obtained sintered compacts are characterized by a relative density ranging between 95.60 and 97.99%. The samples with the lowest and the highest density were SPSed at 400°C/min and 10 min, whereas the compacts SPSed at 50 MPa have the lowest density and those SPSed at 80 MPa the highest density. Generally, doubling the heating rate caused a slight increase in density. What is clearly shown is that both the compacting pressure and holding time play the main role in the densification of the WC-5Co powder mixture, especially when the compacting pressure of 80 MPa was applied. SPS at 50 MPa is not as effective as at 80 MPa. SPS at 80 MPa caused a stable increase in density with an increasing holding time and to a lesser extent the heating rate. Increasing the holding time from 5 to 10 min, when the heating rate of

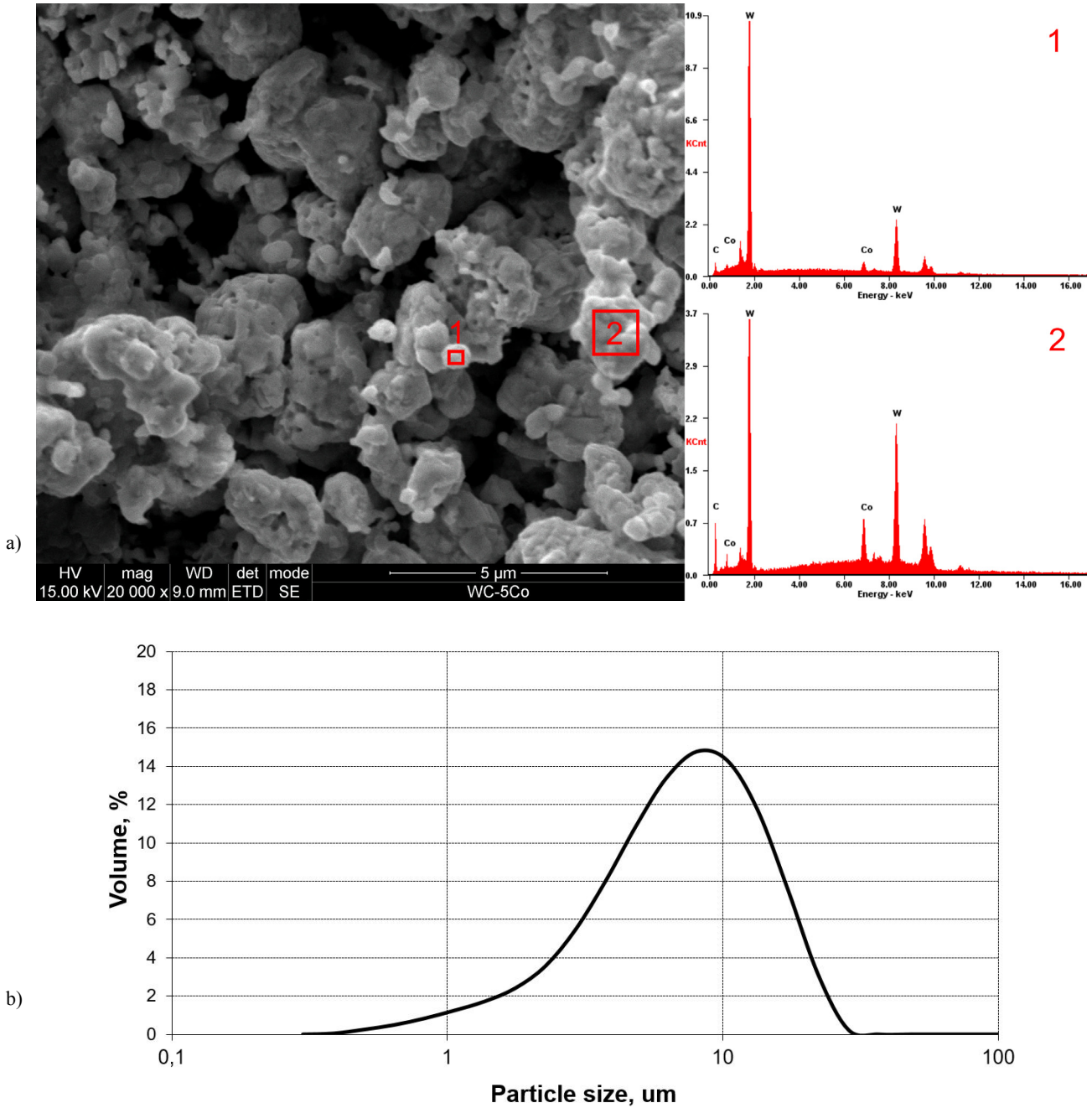


Fig. 2. Powder particles morphology (a) and particle size distribution (b) of WC-5Co powder mixture

200°C/min was applied, caused an increase in the relative density by 0.41%, and by 1.17% at the heating rate of 400°C/min. Using a holding time of 5 min and doubling the heating rate raised the density by 0.08%. In turn, when the holding time was 10 min, the increase in relative density was higher (0.84%). It means that combining a longer holding time and higher rate of heating results in a higher rate of densification, notably when a higher compacting pressure is applied.

For a better understanding of the phase reactions during SPS, X-ray structural studies were performed. The obtained spectra are shown in Fig. 3. In all the cases, the hexagonal WC ceramic phase is clearly visible in the spectrum. The cubic Co binder phase is not always visible in the spectrum, which is often encountered, because X-ray is not sensitive to Co [46]. What

TABLE 1
Properties of SPSed WC-5Co cemented carbides

| CP / HR / HT | Apparent density, g/cm ³ | Relative density, % | Hardness, HV ₃₀ | Fracture toughness (K _{1c}), MPa·m ^{1/2} | WC crystallite size, nm |
|---------------|-------------------------------------|---------------------|----------------------------|---|-------------------------|
| 50 / 200 / 5 | 14.71 | 97.49 | 1806 ±20 | 8.56 ±0.17 | 40 |
| 50 / 200 / 10 | 14.65 | 97.06 | 1754 ±10 | 8.91 ±0.05 | 33 |
| 50 / 400 / 5 | 14.76 | 97.80 | 1771 ±9 | 9.06 ±0.11 | 40 |
| 50 / 400 / 10 | 14.43 | 95.60 | 1754 ±12 | 8.38 ±0.41 | 33 |
| 80 / 200 / 5 | 14.60 | 96.74 | 1780 ±16 | 9.46 ±0.08 | 38 |
| 80 / 200 / 10 | 14.66 | 97.15 | 1797 ±10 | 9.24 ±0.11 | 33 |
| 80 / 400 / 5 | 14.61 | 96.82 | 1861 ±10 | 9.30 ±0.24 | 33 |
| 80 / 400 / 10 | 14.64 | 97.99 | 1789 ±17 | 9.95 ±0.28 | 40 |

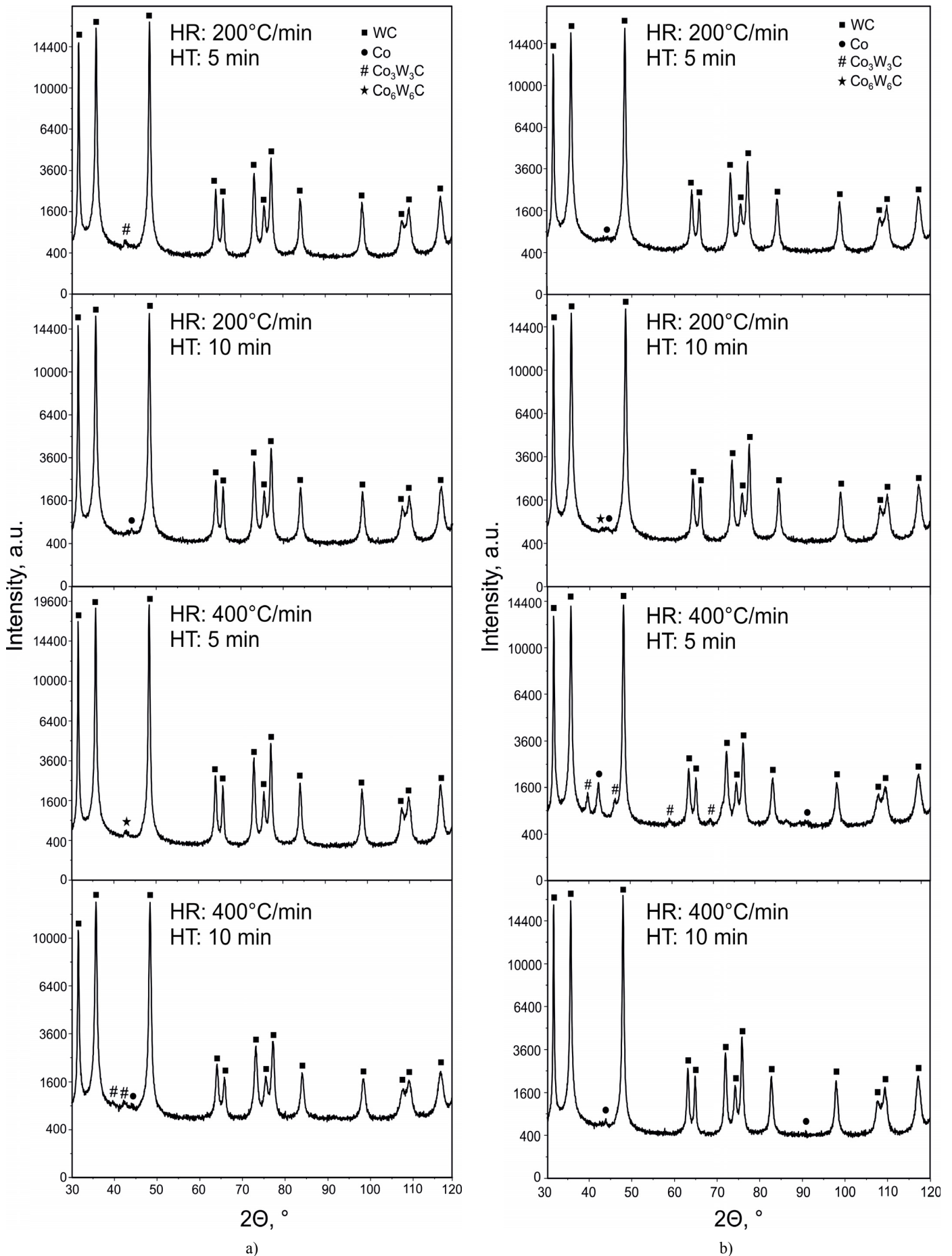
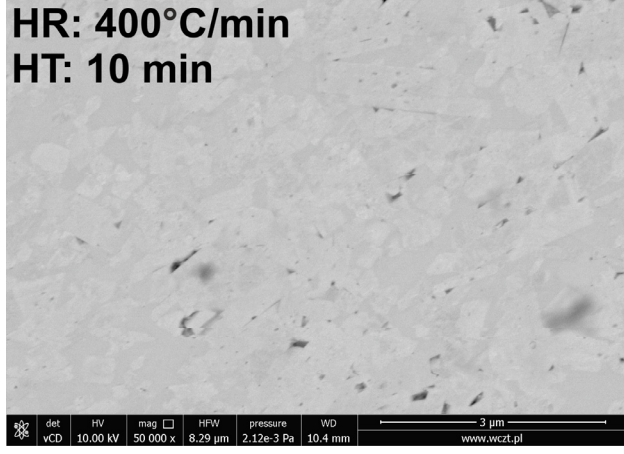
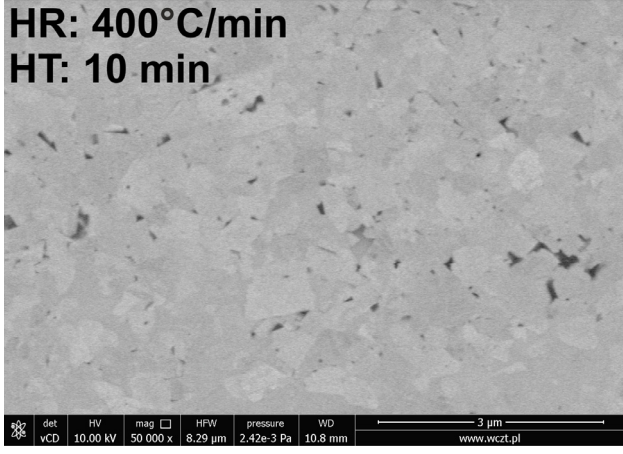
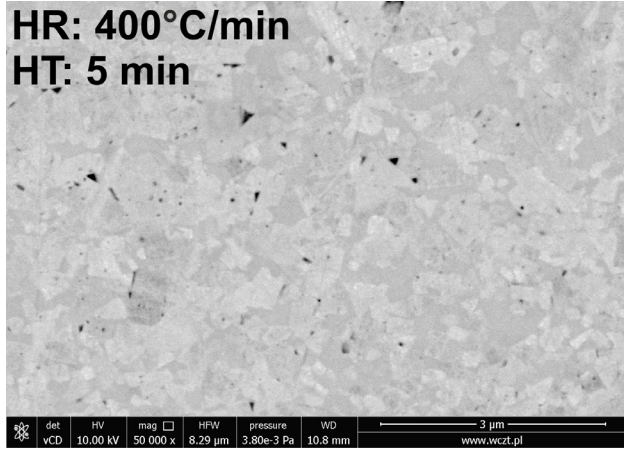
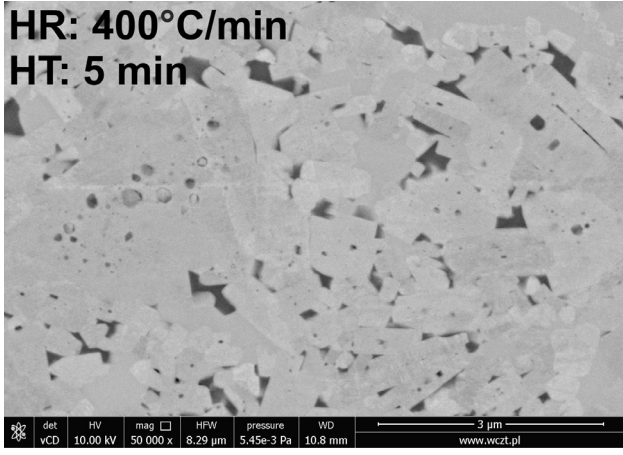
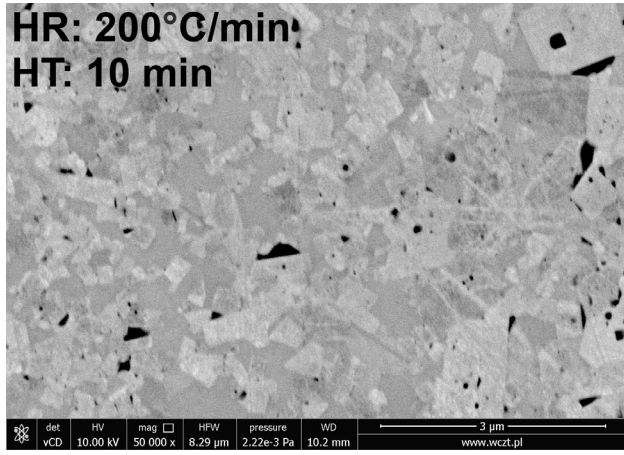
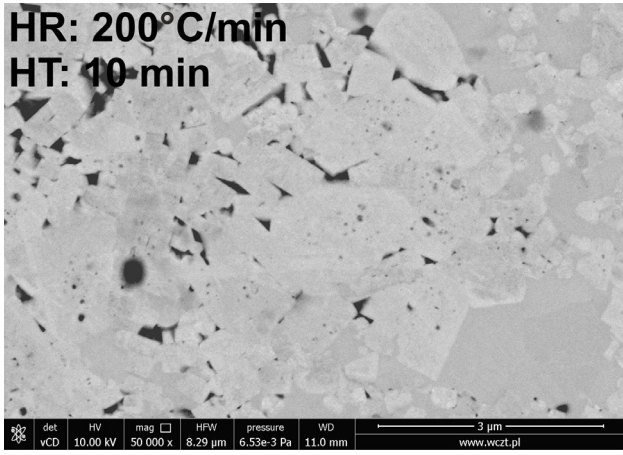
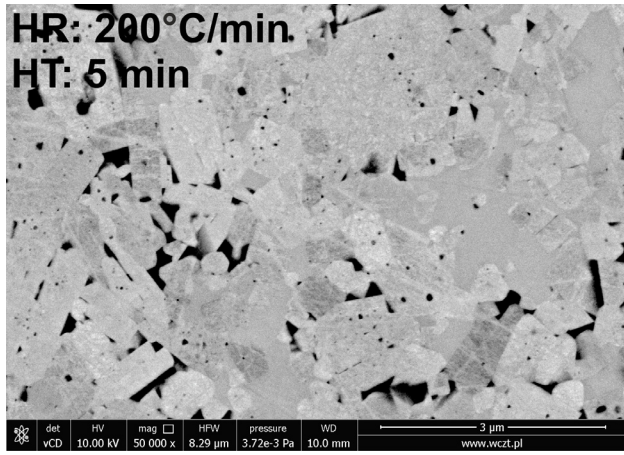
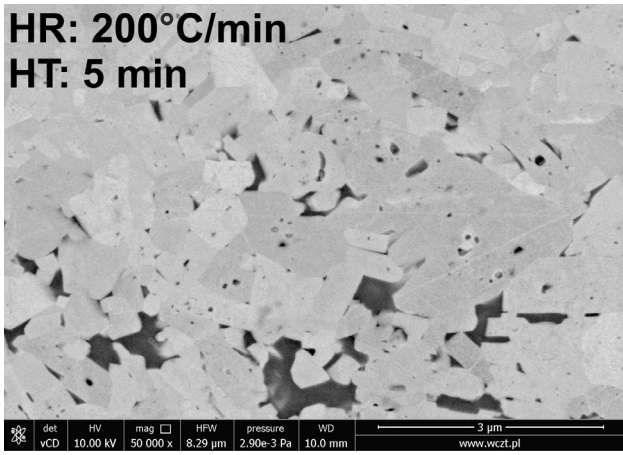


Fig. 3. Diffraction patterns of WC-5Co cemented carbides SPSeD at compacting pressure (CP) of (a) 50 MPa and (b) 80 MPa



a)

b)

Fig. 4. Microstructure of WC-5Co cemented carbides SPSed at compacting pressure (CP) of (a) 50 MPa and (b) 80 MPa

is more important, the X-ray results indicated that during SPS decarburization of the WC grains occurred in a few cases and the cubic η complex phases, $\text{Co}_3\text{W}_3\text{C}$ (ICDD 00-006-0639) as well as $\text{Co}_6\text{W}_6\text{C}$ (ICDD 00-022-0597) were synthesized. The presence of these phases in the microstructure is in agreement with the change in the mechanical properties, where a rise in hardness and fall in fracture toughness are observed. They are related to the high hardness and low toughness of these phases [47]. The η phases, widely recognized as undesirable in WC-Co cemented carbides [48], in this study do not significantly reduce the fracture toughness. This is one example of the superiority of the SPS technique in comparison with conventional sintering of WC-Co cemented carbides, where the presence of secondary phases significantly reduces the toughness [49] and the produced tools would be brittle.

The microstructure of the SPSed WC-5Co cemented carbides is presented in Fig. 4. The analysis of microstructure showed that the bright contrast phase is the WC ceramic and the dark grey contrast phase is the Co binder. Residual porosity is also seen as a black irregular shape in small areas. The WC crystallite size in all the SPSed compacts estimated by the Sherrer method ranged between 33 and 40 nm. A small increase of WC crystallite size seems to be a result of low sintering temperature (1200°C), rapid heating (200 and 400°C min) and short holding time (5 and 10 min) of the powder being sintered. Contrary, in accordance with Zhao et al. [50] SPS of nanometric WC powder (40-70 nm) resulted in increase of WC grain size up to 254 and 305 nm at 1500°C and 1750°C respectively.

The hardness and fracture toughness of SPSed WC-5Co cemented carbides are listed in Table 1. The hardness of all sintered compacts is more than 1750 HV₃₀. The WC-5Co cemented carbides without the presence of η phases in their microstructure are characterized by hardness ranging between 1754 ± 10 and 1797 ± 10 HV₃₀. When the microstructure contains the hard η phase, the hardness is higher than that of previous case (between 1780 ± 16 and 1861 ± 10 HV₃₀). However, the compact SPSed at 50 MPa, 400°C/min, with a 10 min HT exhibits the hardness of 1754 ± 12 HV₃₀ and the fracture toughness of 8.38 ± 0.41 MPa·m^{1/2}. In this case, the low fracture toughness of the composite seems to be effect of low density and the presence of a brittle $\text{Co}_3\text{W}_3\text{C}$ complex phase. In other samples where η phases were synthesized, the fracture toughness is also lower (between 8.56 ± 0.17 MPa·m^{1/2} and 9.30 ± 0.24 MPa·m^{1/2}). In comparison, the fracture toughness of specimens with a microstructure consisting of only WC ceramic embedded in the Co binder ranges between 8.91 ± 0.05 and 9.95 ± 0.28 MPa·m^{1/2}. What is important from the industrial point of view, the obtained WC-5Co cemented carbides have a higher hardness while maintaining the same fracture toughness with respect commercially available cutting inserts, e.g. the H10 (Sandvik) cutting insert from the ISO K10 group having the composition of WC-6Co, whose hardness is 1695 ± 11 HV₃₀ and fracture toughness is 9.31 ± 0.07 MPa·m^{1/2}.

4. Conclusions

WC-5Co cemented carbides were fabricated by SPS using various process parameters (compacting pressure, heating rate and holding time). The best relation of hardness (1861 ± 10 HV₃₀) and fracture toughness (9.30 MPa·m^{1/2}) of WC-5Co cemented carbides was obtained by SPS at 80 MPa, 400°C/min with a holding time of 5 min. The microstructure of this composite material consists of a WC ceramic phase, Co binder phase and synthesized hard and brittle $\text{Co}_3\text{W}_3\text{C}$ complex phase. What is important, the synthesized η phases, widely recognized as undesirable in WC-Co cemented carbides, in these cases do not significantly reduce the investigated mechanical properties, especially fracture toughness. It is clearly seen that the SPS technique allows one to fabricate materials with better mechanical properties than using conventional powder metallurgy techniques. Now, the main limitation of SPS is the production scale. In this study, new graphite tools were designed and produced to fabricate a semi-finished product from which nine cutting inserts were obtained in one SPS process. This approach could be useful for the semi-industrial fabrication of WC-Co cemented carbides cutting inserts using a laboratory scale SPS furnace.

Acknowledgement

The research studies were co-financed by The National Centre for Research and Development as part of the project no. POIR.01.01.01-00-0267/16 entitled "Fabrication of innovative electrodes for heating and hardening of wire tools for machining of hard materials from spark plasma sintered nanocrystalline WC-Co powders".

Correspondence address: Dariusz Garbiec, Metal Forming Institute, 14 Jana Pawla II Street, 61-139 Poznan, dariusz.garbiec@inop.poznan.pl

REFERENCES

- [1] Z. Zhao, *Scripta Mater.* **120**, 103-106 (2016).
- [2] G. Zhang, H. Chen, L. Dong, Y. Yin, K. Li, *Ceram-Silikaty.* **60** (1), 85-90 (2016).
- [3] H. Xie, X. Song, F. Yin, Y. Zhang, *Sci. Rep.* **6** (31047), 1-8 (2016).
- [4] E.O. Hall, *P. Phys. Soc.* **64** (9), 747-752 (1951).
- [5] N.J. Petch, *J. Iron Steel Inst.* **174**, 25-28 (1953).
- [6] W. Liu, X. Song, J. Zhang, F. Yin, G. Zhang, *J. Alloy. Compd.* **458** (1), 366-371 (2008).
- [7] H.-C. Kim, I.-J. Shon, J.-K. Yoon, J.-M. Doh, *Int. J. Refract. Met. H.* **25** (1), 46-52 (2007).
- [8] W. Su, Y.-X. Sun, H.-L. Yang, X.-Q. Zhang, J.-M. Ruan, *T. Non-ferr. Metal Soc.* **25** (4), 1194-1199 (2015).
- [9] Y. Pristinskiy, N. Peretyagin, N.W. Solis Pinargote, *Journal.* **129** (02028), 1-4 (2017).
- [10] P. Siwak, D. Garbiec, M. Rogalewicz, *Mater. Res-Ibero-Am. J.* **20**, 780-785 (2017).

- [11] L. Espinosa-Fernández, A. Borrell, M.D. Salvador, C.F. Gutierrez-Gonzalez, *Wear*. **307** (1), 60-67 (2013).
- [12] P. Siwak, D. Garbiec, T. Nonferr. Metal Soc. **26** (10), 2641-2646 (2016).
- [13] O.O. Ige, S. Aribo, B.A. Obadele, T. Langa, K.M. Oluwasegun, M.B. Shongwe, P.A. Olubambi, *Int. J. Refract. Met. H.* **66**, 36-43 (2017).
- [14] M.R. Rumman, Z. Xie, S.-J. Hong, R. Ghomashchi, *Mater. Design*. **68**, 221-227 (2015).
- [15] Y. Liu, J. Cheng, B. Yin, S. Zhu, Z. Qiao, J. Yang, *Tribol. Int.* **109**, 19-25 (2017).
- [16] R.M. Raihanuzzaman, M. Rosinski, Z. Xie, R. Ghomashchi, *Int. J. Refract. Met. H.* **60**, 58-67 (2016).
- [17] S. Lee, H.S. Hong, H.-S. Kim, S.-J. Hong, J.-H. Yoon, *Int. J. Refract. Met. H.* **53**, 41-45 (2015).
- [18] P.A. Olubambi, K.K. Alaneme, A. Andrews, *Int. J. Refract. Met. H.* **50**, 163-177 (2015).
- [19] N. Al-Aqeeli, *Powder Technol.* **273**, 47-53 (2015).
- [20] N. Al-Aqeeli, K. Mohammad, T. Laoui, N. Saheb, *Ceram. Int.* **40** (8 Part A), 11759-11765 (2014).
- [21] V. Bonache, M.D. Salvador, V.G. Rocha, A. Borrell, *Ceram. Int.* **37** (3), 1139-1142 (2011).
- [22] L. Sun, T.E. Yang, C. Jia, J. Xiong, *Int. J. Refract. Met. H.* **29** (2), 147-152 (2011).
- [23] S. Zhao, X. Song, C. Wei, L. Zhang, X. Liu, J. Zhang, *Int. J. Refract. Met. H.* **27** (6), 1014-1018 (2009).
- [24] I.F. Machado, L. Girardini, I. Lonardelli, A. Molinari, *Int. J. Refract. Met. H.* **27** (5), 883-891 (2009).
- [25] J.A. Picas, Y. Xiong, M. Punset, L. Ajdelsztajn, A. Forn, J.M. Schoenung, *Int. J. Refract. Met. H.* **27** (2), 344-349 (2009).
- [26] X. Liu, X. Song, J. Zhang, S. Zhao, *Mat. Sci. Eng. A-Struct.* **488** (1), 1-7 (2008).
- [27] L. Sun, C. Jia, R. Cao, C. Lin, *Int. J. Refract. Met. H.* **26** (4), 357-361 (2008).
- [28] L. Krüger, K. Mandel, R. Krause, M. Radajewski, *Int. J. Refract. Met. H.* **51**, 324-331 (2015).
- [29] S. Zhao, X. Song, J. Zhang, X. Liu, *Mat. Sci. Eng. A-Struct.* **473** (1), 323-329 (2008).
- [30] L. Sun, C.-C. Jia, C.-G. Lin, R.-J. Cao, *J. Iron Steel Res. Int.* **14** (5, Supplement 1), 85-89 (2007).
- [31] B. Yaman, H. Mandal, *Mater. Lett.* **63** (12), 1041-1043 (2009).
- [32] K. Mandel, L. Krüger, R. Krause, M. Radajewski, *Int. J. Refract. Met. H.* **47** 124-130 (2014).
- [33] W.-H. Chen, H.-T. Lin, P.K. Nayak, J.-L. Huang, *Ceram. Int.* **40** (9, Part B), 15007-15012 (2014).
- [34] C.-C. Jia, H. Tang, X.-Z. Mei, F.-Z. Yin, X.-H. Qu, *Mater. Lett.* **59** (19), 2566-2569 (2005).
- [35] K. Mandel, M. Radajewski, L. Krüger, *Mat. Sci. Eng. A-Struct.* **612**, 115-122 (2014).
- [36] F. Zhang, J. Shen, J. Sun, *Mat. Sci. Eng. A-Struct.* **381** (1), 86-91 (2004).
- [37] B. Yaman, H. Mandal, *Int. J. Refract. Met. H.* **42**, 9-16 (2014).
- [38] C.B. Wei, X.Y. Song, J. Fu, X.M. Liu, Y. Gao, H.B. Wang, S.X. Zhao, *Mat. Sci. Eng. A-Struct.* **552**, 427-433 (2012).
- [39] S.G. Huang, L. Li, K. Vanmeensel, O. Van der Biest, J. Vleugels, *Int. J. Refract. Met. H.* **25** (5), 417-422 (2007).
- [40] S.G. Huang, K. Vanmeensel, L. Li, O. Van der Biest, J. Vleugels, *Int. J. Refract. Met. H.* **26** (3), 256-262 (2008).
- [41] S.I. Cha, S.H. Hong, B.K. Kim, *Mat. Sci. Eng. A-Struct.* **351** (1), 31-38 (2003).
- [42] X. Sun, Y. Wang, D.Y. Li, *Wear*. **301** (1-2), 406-414 (2013).
- [43] V. Bonache, M.D. Salvador, A. Fernández, A. Borrell, *Int. J. Refract. Met. H.* **29** (2), 202-208 (2011).
- [44] R.M. Raihanuzzaman, T.S. Jeong, R. Ghomashchi, Z. Xie, S.-J. Hong, *J. Alloy. Compd.* **615**, S564-S568 (2014).
- [45] W.D. Schubert, H. Neumeister, G. Kinger, B. Lux, *Int. J. Refract. Met. H.* **16** (2), 133-142 (1998).
- [46] R. Jenkins, R.L. Snyder, *Introduction to X-ray Powder Diffraction*, Wiley Online Library (1996).
- [47] F.C.M.A. Formisano, A. Caraviello, L. Carrino, M. Durante, A. Langella, *Advances in Tribology*. **2016** (5063274), 1-6 (2016).
- [48] O. Eso, Z.Z. Fang, A. Griffio, *Int. J. Refract. Met. H.* **25** (4), 286-292 (2007).
- [49] J.A. Gurland, *T. Am. I. Min. Met. Eng.* **200**, 285-290 (1954).
- [50] J. Zhao, T. Holland, C. Unuvar, Z.A. Munir, *Int. J. Refract. Met. H.* **27** (1), 130-139 (2009).